RSC Advances

PAPER

View Article Online
View Journal | View Issue

Cite this: *RSC Adv.*, 2016, **6**, 98956

Palladium(II) tetrasulfophthalocyanine covalently immobilized on keratin protein grafted graphene oxide nanosheets as a new high-performance catalyst for C–C coupling reactions

Zeinab Hezarkhani and Ahmad Shaabani*

Received 24th July 2016
Accepted 10th October 2016

DOI: 10.1039/c6ra18814a

www.rsc.org/advances

Wool keratin protein, as an amphiphilic biomaterial, was extracted from natural wool and used to modify the surface of graphene oxide nanosheets. An aqua soluble palladium(II) complex with a phthalocyanine ligand possessing the ability to covalently bind on keratin-protein-grafted graphene oxide nanosheets was used to chemically attach palladium(II) complex to modified graphene oxide. The covalently supported palladium(II) tetrasulfophthalocyanine complex revealed efficient catalytic reactivity by controlled temporary release of active species for Heck and Sonogashira coupling reactions in aqueous solution. Heck coupling of styrene and Sonogashira coupling of phenylacetylene with different aryl halides were successfully catalyzed by the synthesized palladium(II) tetrasulfophthalocyanine covalently supported on keratin-protein-grafted graphene oxide nanosheets as a novel catalyst precursor. The controlled release of palladium active species prevents the formation of inactive palladium agglomerates under harsh conditions and consequently this controlled release leads to high catalytic performances.

Introduction

Palladium-catalyzed cross-coupling reactions as extraordinary powerful and widespread methods are found in all areas of chemistry which construct carbon–carbon and carbon–heteroatom bonds.[1–8] The palladium-catalyzed formation of C–C bonds is typically associated with "ligandless" palladium species released from homogeneous and heterogeneous catalysts in the reaction solution. Since irreversible precipitation of palladium in the reaction media affects its catalytic activities, to settle the matter, a controlled and reversible release of palladium from macrocyclic complexes, as a novel method, was proposed.[9–13] The interplay between the release and recoordination of Pd in the presented new concept is the reason for the high catalytic performances of macrocyclic Pd complexes as precatalysts in C–C coupling reactions. Kostas *et al.* have reported the use of a water-soluble Pd porphyrin precatalyst for the Suzuki reaction in water.[9] Wan *et al.* have used a Pd porphyrin as a catalyst precursor for the Heck reaction in ionic liquids as the reaction medium.[10] The use of a macrocyclic Robson-type complex of Pd as the precatalyst in the Heck reaction was reported by Röhlich and Köhler.[11] Also, Röhlich and Köhler reported that homeopathic Pd concentration in solution released from macrocyclic Pd complexes leads to high C–C coupling activity in Heck and Suzuki reactions.[12]

The immobilization of a homogeneous palladium complex catalyst onto a solid facilitates the separation of the catalyst and improves its catalytic activity. Recently, the covalent immobilization of palladium complexes onto graphene oxide using different ligands such as N-heterocyclic carbenes,[14–16] *N*-aminoguanidine,[17] aminosilane ligand spacer,[18] nitrogen bidentate ligand,[19] and ring-opening metathesis polymerization-derived polymers[20] were reported for the various C–C coupling reactions. These systems were showed improved catalytic activity and high recyclability without any decrease in activity.

Palladium phthalocyanines (PdPcs), as precursors for the Pd(II) oxidation state, exhibit very high thermal and chemical stability. The central palladium atom in phthalocyanine ligand of PdPcs is completely coordinatively saturated. Since PdPcs possess an extraordinarily high complex stability, the release of Pd under coupling reaction conditions would be very limited. Due to the very rigid structure of phthalocyanine ligand in PdPcs, they cannot dissociate partially and thus Pd released by them would be "completely unsaturated". Because the release of palladium from its phthalocyanine complex is reversible,[13] the phthalocyanine ligand has mainly the task of avoiding the deactivation of the released palladium species. Thus, PdPcs can be very applicable systems for C–C coupling reactions and the released palladium species that are formed *in situ* from the PdPc precursor have the highest activity. Recently, it was reported that organometallic compounds with a π-electron system like metal phthalocyanine can be adsorbed/intercalated (onto/into graphene layers),[21,22] and/or

Faculty of Chemistry, Shahid Beheshti University, G. C., P. O. Box 19396-4716, Tehran, Iran. E-mail: a-shaabani@sbu.ac.ir

chemically attached[23,24] to graphene-based materials to pointedly enhance their performance.

Natural biopolymers have highly specialized properties such as inspiring morphologies, complex three-dimensional structures, biocompatibility, and biodegradability. Because of the attractive features of natural biopolymers, these materials have superior performances as a choice for nanocomposites.[25–28] Wool is a fibrous protein that composed of approximately 95 wt% pure keratin protein.[29] The keratin protein has different kinds of the amino acids that between them the cysteine can be found in high concentration. The high amount of the cysteine and the presence of amino acids like serine, threonine, arginine, and lysine makes it possible to attach different compounds chemically, by using the nucleophilic substitution reactions because of the presence of the –OH and $-NH_2$ functional groups in the mentioned amino acids. Due to the presence of amino acid chains in the keratin protein, the mentioned protein can react with functional complexes of metals and suitable supports; therefore, keratin protein can be used as a linker for the attaching of catalysts to the supports. So, extraction of keratin protein from natural wool would be a useful method for the synthesis of catalytic systems. Because of the presence of strong disulfide bonds, inter- and intramolecular bonding of polar and nonpolar amino acids, and α-helices structure of polypeptide in wool keratin, this protein shows resistance to degradation in common solvents and it is insoluble in water, dilute acids, alkalis, and organic solvents. Solubilisation of wool proteins to produce useful materials can be achieved using reduction,[30–32] oxidation,[32–34] sulfitolysis of the disulfide bonds,[30,35,36] and dissolution techniques by ionic liquids and deep eutectic solvents.[29]

Interest in graphene oxide (GO) in the fields of nanochemistry and catalysis stems from its unique properties such as high thermal and mechanical stability, high water dispersibility, high surface area, easy surface modifications, and oxygen-carrying functionalities. These properties make graphene oxide a promising material for the immobilization of catalysts.[37–39] Recently, graphene oxide nanosheets have been modified with various natural polymers such as chitosan,[40] starch,[41] cellulose,[42] regenerated silk fibroin,[25] and keratin obtained from chicken feathers,[43] providing them with interesting new properties. Functionalization of graphene to manipulate its interfacial property is of significant importance in catalytic chemistry.[44] Functionalization of graphene can improve the grafting or loading of supported catalysts. Natural proteins, as amphiphilic biomaterials, are well-known as "adhesive" to link hydrophobic and hydrophilic substrates.[44] The keratin protein has –OH and $-NH_2$ functional groups that can be used to chemically attach different compounds using the nucleophilic substitution reaction. Therefore, because of chemical inertness of graphene oxide to form catalyst–graphene interactions, we used keratin protein of natural wool as a modifier to covalently link graphene oxide and water-soluble palladium(II) tetrasulfophthalocyanine (PdTSPc). By immobilization of PdTSPc onto modified graphene oxide, the recyclable catalyst can be obtained with improved catalytic utility and activity.

During the course of our studies toward the synthesis of phthalocyanines[45] and introduction of new catalysts for the organic transformations,[23,24,46–48] herein, palladium(II) tetrasulfophthalocyanine supported on keratin-protein-grafted graphene oxide nanosheets (PdTSPc@KP–GO) was synthesized and its catalytic activity was investigated in Heck coupling of styrene and Sonogashira coupling of phenylacetylene with different aryl halides in water as reaction media. PdTSPc@KP–GO is prepared as Scheme 1.

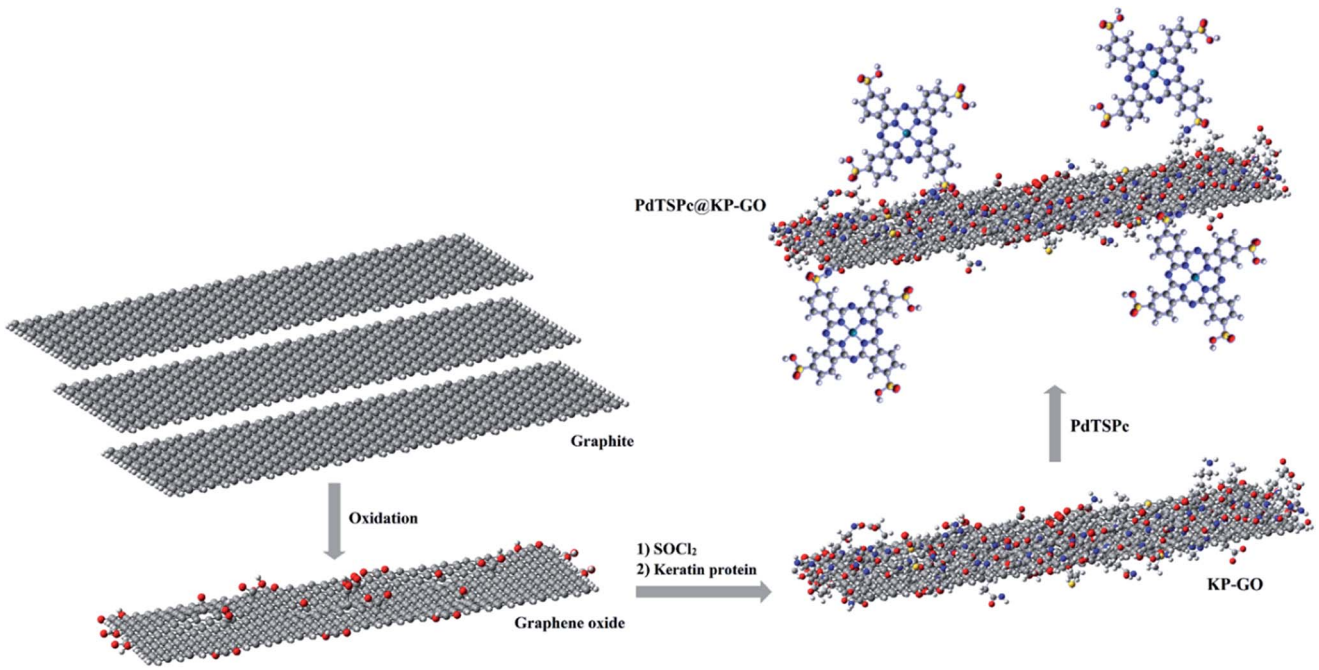

Scheme 1 Preparation of PdTSPc@KP–GO.

Materials and methods

1 General

Natural white wool (sheep of Kangavar/Iran) was washed with NaOH solution, distilled water, and methanol, and then cut into very short pieces. All reagents were obtained from Aldrich or Merck and used without further purification. Palladium determination was carried out on a FAAS (Shimadzu model AA-680 flame atomic absorption spectrometer with a Pd hollow cathode lamp at 244.8 nm, using an air-acetylene flame) and inductively coupled plasma optical emission spectrometer (ICP-OES) Varian Vista PRO Radial. UV-vis spectra were recorded employing an Analytik Jena Specord S600 Diode Array spectrometer. FT-IR spectra were recorded on a Shimadzu IR-470 spectrometer. X-ray diffraction (XRD) pattern of catalyst was recorded on a STOE STADI P with scintillation detector, secondary monochromator using Cu Kα radiation ($\lambda = 0.1540$ nm). Thermogravimetric analysis (TGA) was carried out using STA 1500 instrument at a heating rate of 10 °C min^{-1} in the air. Scanning electron microscopy (SEM) observations were carried out on a scanning electron microscope (TESCAN Vega Model). All samples were sputtered with gold before observation. Transmission Electron Microscopy (TEM) characterization was performed using a transmission microscope Philips CM-30 with an accelerating voltage of 150 kV. X-ray photoelectron spectroscopy (XPS) analysis was performed using a Gammadata-scienta ESCA 200 hemispherical analyzer equipped with an Al Kα (1486.6 eV) X-ray source. Raman spectra were recorded on a Bruker SENTERR (2009) with an excitation beam wavelength at 785 nm. Microwave irradiation experiment was carried out in a Microsynth Milestone SRL microwave apparatus. Substances were identified and quantified by a Varian 3900 GC.

2 Experimental: synthesis of palladium(II) tetrasulfophthalocyanine supported on keratin protein grafted graphene oxide nanosheets (PdTSPc@KP–GO)

Pd(II) tetrasulfophthalocyanine (PdTSPc) supported on keratin-protein-grafted graphene oxide nanosheets (KP–GO) is prepared as Scheme 1.

2.1 Synthesis of palladium(II) tetrasulfophthalocyanine (PdTSPc). The synthesis of PdTSPc was done inspired by previously reported procedures for synthesis of metal(II) phthalocyanines (MPcs)[45,49] and the sulfonation of the MPcs,[50] as following: the palladium(II) phthalocyanine (PdPc) was synthesized by controlled microwave heating of homogeneous powder containing of phthalic anhydride (0.88 g, 6.0 mmol), urea (1.6 g, 26 mmol), Pd(II) chloride (0.32 g, 1.8 mmol), and ammonium heptamolybdate (0.02 g, 0.02 mmol) that were grounded together. The obtained mixture was irradiated at 130 °C for 10 min. The crude product was purified using the method reported in the mentioned references and the final PdPc dried in vacuum at 80 °C. Palladium trisulfophthalocyanine sulfonyl chloride was produced by heating the synthesized PdPc (1.0 mmol) with chlorosulfonic acid (7.0 mmol) in 1,2,4-trichlorobenzene (50 mL) at 180–190 °C for 2 h.

2.2 Synthesis of graphene oxide (GO). GO was synthesized by a modified Hummers method.[51,52] The graphite powder (1.0 g) was added to a round-bottom flask containing a mixture of $K_2S_2O_8$ (1.0 g) and P_2O_5 (1.0 g) in concentrated H_2SO_4 (6.0 mL). The mixture of the reaction was stirred for 6 h at 80 °C. Deionized water (DI water, 200 mL) was added to the cooled mixture and stirred overnight. After filtration of the mixture, the residue was washed with DI water and dried overnight to give the preoxidized graphite. To a round-bottom flask containing concentrated H_2SO_4 (50 mL) at 0 °C, the as-prepared preoxidized graphite powder was added and stirred for 10 min. $KMnO_4$ (6.0 g) was added to the mixture and the mixture of reaction stirred at room temperature. After 4 h, the reaction flask was placed in an ice bath and DI water (400 mL) in two steps (at first 100 mL and after 2 h, 300 mL) was added to the mixture. After that, by dropwise addition of 30% H_2O_2 to the mixture of reaction, the color of the reaction mixture changed into yellow. The mixture of the reaction was filtered and the residue was washed with 0.1 M HCl and 300 mL DI water, respectively, and dried in the air.

2.3 Preparation of keratin protein (KP) of natural wool. The dissolution of natural wool fibers was done in 1-butyl-3-methylimidazolium chloride ([BMIM]Cl) at 130 °C for 12 hours under an N_2 atmosphere based on the previously reported method.[29] Briefly, to a magnetically stirred solution of 2-mercaptoethanol (15 mg, 0.2 mmol) in [BMIM]Cl (5.0 g), the natural wool fibres (75 mg) were added during 1 h at 130 °C. The stirring was continued for 12 h until the fibres completely dissolved.

2.4 Synthesis of keratin protein grafted graphene oxide nanosheets (KP–GO). The prepared GO (40 mg) was added to the solution of dry DMF (1.0 mL) in $SOCl_2$ (30 mL). The mixture of the reaction was continuously stirred with a magnetic stirrer at 70 °C for 24 h. After evaporation of the solvent (100 °C); the obtained acylated graphene oxide product (GO–COCl) was washed with dry THF. The product was added to the as-prepared solution of wool keratin protein in the [BMIM]Cl at 80 °C and the mixture was stirred for 12 h. The product was filtered and the residue was washed successively with DI water and ethanol and finally dried at 50 °C under vacuum to give keratin-protein-grafted graphene oxide nanosheets (KP–GO).

2.5 Synthesis of PdTSPc@KP–GO. The as-prepared KP–GO (0.2 g) was added to dry DMF (30 mL) and sonicated until a dispersed mixture was obtained. To a magnetically stirred solution of palladium trisulfophthalocyanine sulfonyl chloride (0.3 mmol) in 50 mL of dry DMF at room temperature, the dispersed KP–GO mixture was added and the temperature is raised to 100 °C. The stirring of reaction media is continued at this temperature for about 24 h until the PdTSPc is substantially supported on the surface of KP–GO. Finally, the mixture was centrifuged and the catalyst was washed with H_2O (3 × 20 mL) and EtOH (3 × 20 mL) in sequence and dried under vacuum at 80 °C.

3 General procedures for catalytic tests

3.1 Heck coupling. Styrene (0.1 g, 1.0 mmol) and an aryl halide (1.5 mmol) were added to a round-bottomed flask containing K_2CO_3 (0.3 g, 2.0 mmol) and dispersed PdTSPc@KP–GO (98 mg) in H_2O (10 mL). The reaction mixture was refluxed with vigorous stirring for the respective reaction time. After

completion, the mixture of the reaction was cooled and filtered to separate PdTSPc@KP–GO as precatalyst. The solvent of the filtrate was evaporated (under vacuum) and the residue was analyzed by GC method (1-dodecane as an internal standard).

3.2 Sonogashira coupling. A mixture of phenylacetylene (0.1 g, 1.0 mmol), an aryl halide (2.0 mmol), and dispersed PdTSPc@KP–GO (123 mg) in 5.0 mL of H_2O and a solution of K_2CO_3 (0.3 g, 2.0 mmol) and CuI (4.0 mol%) in 5.0 mL of H_2O were prepared, separately. In continue, the solution of K_2CO_3 and CuI were added to the mixture of phenylacetylene, aryl halide, and PdTSPc@KP–GO. The mixture of the reaction was stirred under reflux conditions for the indicated time in Table 2. The mixture was cooled to room temperature. After separation of PdTSPc@KP–GO precatalyst and evaporation of the filtrate solvent under vacuum, the residue was analyzed by GC method (1-dodecane as an internal standard).

Results and discussion

After preparation of GO and palladium trisulfophthalocyanine sulfonyl chloride, extraction of keratin protein from natural wool, and subsequently surface modification of GO by keratin protein of wool, PdTSPc@KP–GO was synthesized by simple mixing of the palladium trisulfophthalocyanine sulfonyl chloride with keratin-protein-grafted graphene oxide. The Pd content of the PdTSPc@KP–GO precatalyst was determined using flame atomic absorption spectrometry (FAAS) method. The amount of Pd in the PdTSPc@KP–GO precatalyst was obtained 0.86%. Inductively coupled plasma optical emission spectrometry (ICP-OES) corroborates the amount of Pd in the PdTSPc@KP–GO determined using FAAS method. In addition, the amount of PdTSPc in the PdTSPc@KP–GO was measured using UV-vis method (Fig. 1). To do that, PdTSPc@KP–GO was dissolved in H_2SO_4 (5.0 mL) with sonication and then the total volume of the solution made up to about 50 mL with H_2O. In continue, the concentration of Pd(II) tetrasulfophthalocyanine was determined using calibration curves of prepared PdTSPc solution standards. The obtained result using UV-vis method was consistent with the result of FAAS and ICP-OES methods.

The energy dispersive spectroscopy (EDS) analysis was used to determine the chemical composition of PdTSPc@KP–GO, which proves the presence of nitrogen, sulfur, and palladium in the mentioned precatalyst (Fig. 2).

The cysteine, serine, threonine, arginine, and lysine of the keratin protein, which have –OH and $–NH_2$ functional groups can participate in the nucleophilic substitution reaction with the –COCl group of the acylated graphene oxide (GO–COCl) and the $–SO_2Cl$ group of the palladium trisulfophthalocyanine sulfonyl chloride to produce KP–GO and PdTSPc@KP–GO, respectively. The covalent interactions between GO, keratin protein, and palladium(II) complex in PdTSPc@KP–GO were indicated by FT-IR method (Fig. 3). FT-IR spectrum of GO reveals characteristic bands at 3375, 1724, 1569, 1384, 1208, and 1049 cm^{-1}, which exhibit the successful synthesis of graphene oxide nanosheets and the presence of oxygenated functional groups on the graphene skeleton: –OH ($\nu = 3375\ cm^{-1}$), carboxyl –C=O and –C–O ($\nu = 1724\ cm^{-1}$ and $1384\ cm^{-1}$ respectively), aromatic –C=C– ($\nu = 1569\ cm^{-1}$), epoxy –C–O ($\nu = 1208\ cm^{-1}$) and alkoxy –C–O ($\nu = 1049\ cm^{-1}$).[53] The chemical attachment of the keratin protein to the GO is confirmed by the presence of the new absorption bands at 2958, 2920, and 2850 cm^{-1} in the IR spectra that are related to the C–H of the CH_2 groups of keratin protein. The elimination of the adsorption band at 1724 cm^{-1} (–C=O of $–CO_2H$ on the graphene oxide skeleton) and formation of the new adsorption band at the 1662 cm^{-1} (–C=O of –CONH–) is confirming the formation of the amide bonds from the reaction between the $–NH_2$ group of keratin protein and –COCl group of acylated GO. Also, the removal of the absorption band at the 1384 cm^{-1} and formation of the new band at the 1446 cm^{-1} that are related to the –C–O of $–CO_2H$ skeleton of the GO and –C–N of –CONH–, respectively is approving the chemically attachment of the keratin protein to GO.

The covalent attachment of the PdTSPc to the KP–GO is confirmed by the observing new adsorption band at the 1375 cm^{-1}, related to the S=O of sulfonamide functional group *via* the reaction between the $–NH_2$ group of the KP–GO and the $–SO_2Cl$ group of the palladium trisulfophthalocyanine sulfonyl chloride.

The thermal stability of PdTSPc@KP–GO precatalyst was examined by thermogravimetric analysis (TGA). The thermograms of GO and PdTSPc@KP–GO are shown in Fig. 4. The main

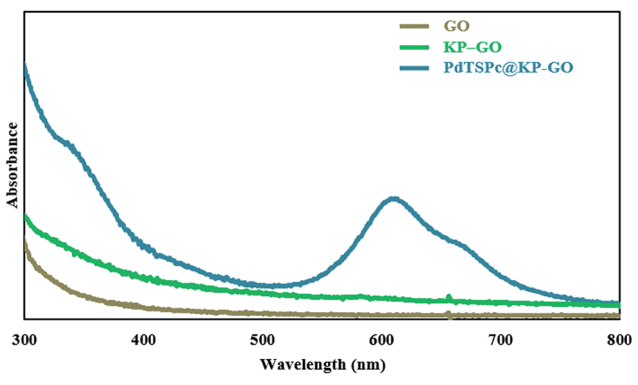

Fig. 1 UV-vis spectrums of GO, KP–GO, and PdTSPc@KP–GO in H_2O : H_2SO_4 (9 : 1).

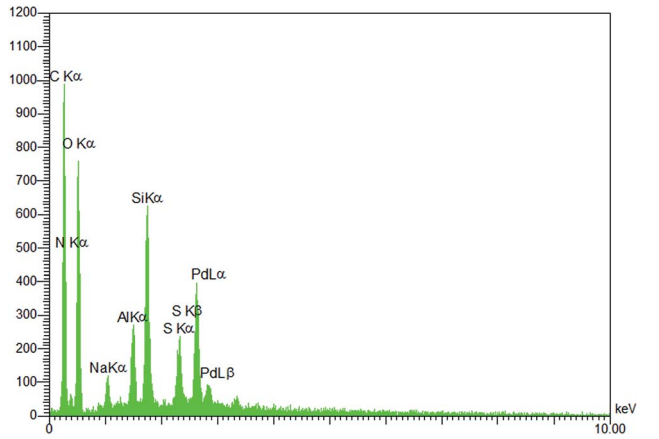

Fig. 2 EDS result for PdTSPc@KP–GO.

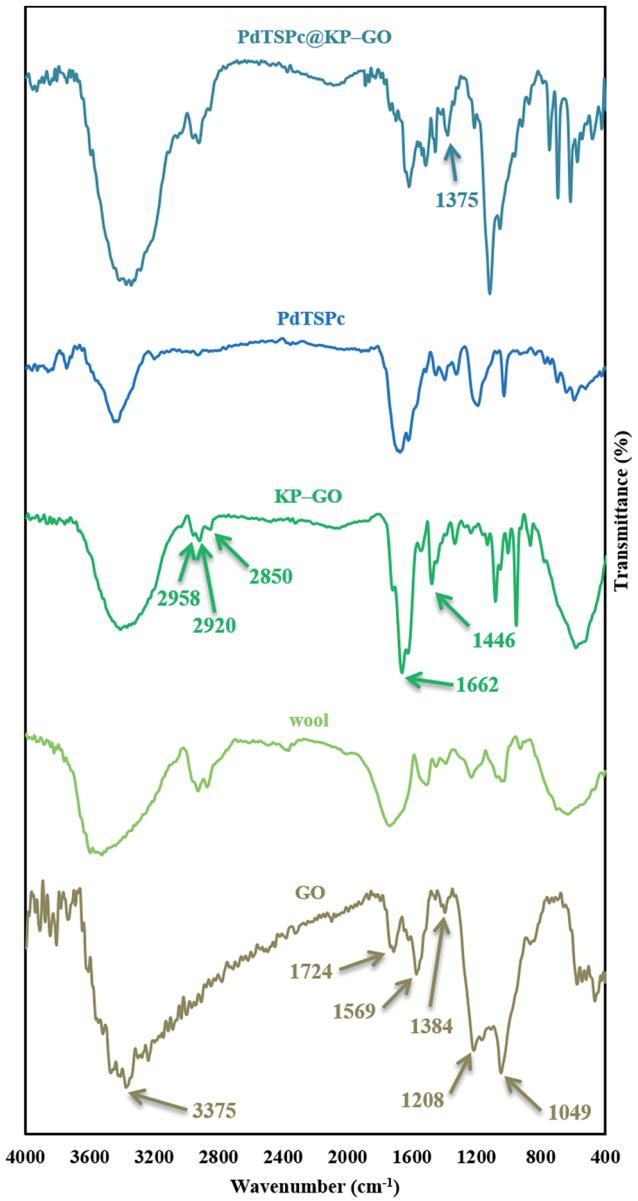

Fig. 3 FT-IR spectra of GO, natural wool, KP–GO, PdTSPc, and PdTSPc@KP–GO.

mass loss of GO takes place above 170 °C, which it should be related to CO, CO_2, and steam release from the thermal decomposition of the most labile oxygen-containing functional groups.[54] The result related to TGA thermogram of PdTSPc@KP–GO revealed the high thermal stability of it. The main decomposition process of PdTSPc@KP–GO occurs in the temperature range of 155–527 °C owing to the decomposition of labile oxygen functional groups of GO support, grafted-keratin-protein, and PdTSPc. PdTSPc@KP–GO becomes thermally more stable than GO during the heating process due to the functionalization of labile oxygen functional groups by keratin protein.

Further characterization of the structure of the catalyst was done using X-ray diffraction (XRD) patterns of GO, natural wool, KP–GO, PdTSPc, and PdTSPc@KP–GO (Fig. 5). The XRD pattern

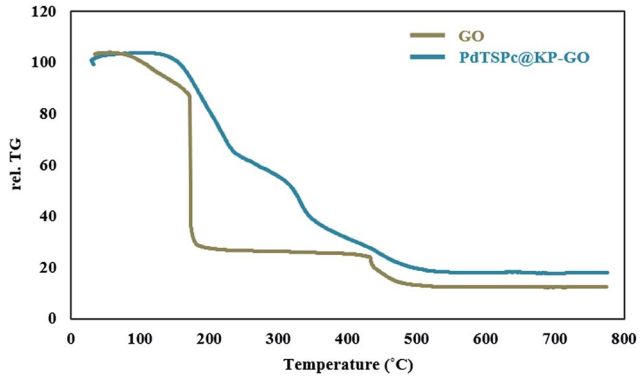

Fig. 4 TG curves of GO and PdTSPc@KP–GO in air.

of graphene oxide nanosheets shows the diffraction peak at $2\theta = 11.3°$ that indicates graphite is oxidized completely. Two broad peaks of natural wool fibers are observed around 2θ of 9° and 21° whereas the wool keratin protein grafted graphene oxide nanosheets manifests peaks at around $2\theta = 9.9°$ and 19.8°. Compared to characteristic diffraction peaks of the natural wool, the XRD pattern for the wool–keratin-protein grafted graphene oxide nanosheets clearly shows the decrease of the peak at about 9° and the enlargement of the peak at about 19.8°; because, the α-helix structure of keratin protein is destroyed during the dissolving process and is not restored.[55] The XRD pattern of PdTSPc indicates the characteristic diffraction peaks at 2θ values of 4.7°, 8.2°, 9.6°, 26.6°, 31.5°, 45.2°, 56.2°, 66.0°, and 74.9°. In the XRD pattern of PdTSPc@KP–GO, the characteristic diffraction peaks at around $2\theta = 9.8°$ and 19.4° are related to the KP–GO. Also, the diffraction peaks of PdTSPc are observable at 2θ values of 26.6°, 31.5°, and 45.2° in the mentioned catalyst. At around $2\theta = 9°$ the diffraction peak of PdTSPc@KP–GO related to the KP–GO are observable; the mentioned peak is stronger than the diffraction peaks of PdTSPc at the same region, therefore, the peaks related to the PdTSPc are not obviously evident. It should be mentioned that in the XRD patterns of GO, natural wool, KP–GO, PdTSPc,

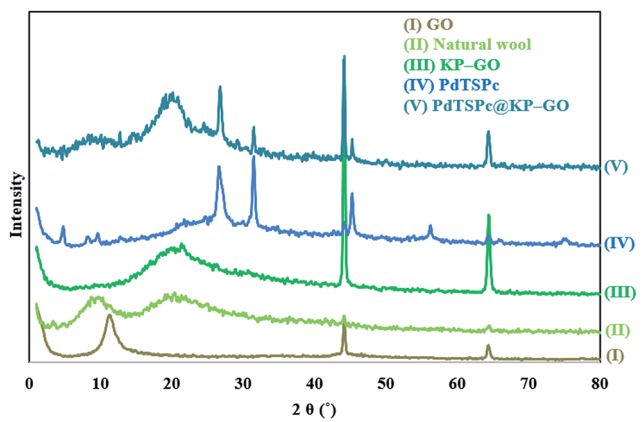

Fig. 5 XRD patterns of GO, natural wool, KP–GO, PdTSPc, and PdTSPc@KP–GO.

and PdTSPc@KP–GO the diffraction peaks at $2\theta = 44^\circ$ and 64° are related to the aluminum sample holder.[56]

The keratin protein was used for the chemical modification of the graphene oxide to make it suitable for the attaching the PdTSPc chemically. To study the structure, morphology, and surface of the prepared material, the scanning electron microscopy (SEM) and transmission electron microscopy (TEM) methods were used (Fig. 6). The SEM image in Fig. 6a shows that the graphene oxide nanosheets are uniform throughout the surface. Although, some wrinkles were detected on the surface of graphene oxide because of the randomly aggregated and crumpled thin nanosheets. As it is seen in representative SEM image of KP–GO (Fig. 6c), it remains as a nanosheet-like structure, but the wrinkles of the KP–GO are more in comparison with the GO due to the presence of the keratin protein. The wrinkles of the final prepared PdTSPc@KP–GO catalyst is much higher (Fig. 6e) than parent KP–GO, because of the addition of the PdTSPc to the system.

The TEM image in the Fig. 6b shows thin layers of GO. In the case of the KP–GO, Fig. 6d, an increase in the layer thickness is observable because of the addition of the keratin protein layer to the GO. By adding the PdTSPc to the KP–GO, the thickness of the prepared catalyst was increased as it is observable in the Fig. 6f.

Phthalocyanine molecules are prone to aggregation, which greatly decreases the active sites of the catalyst. Therefore, by attaching phthalocyanine molecules to large planar graphene oxide sheets, aggregation between the phthalocyanine molecules is prevented during the reaction processes, maintaining isolation between catalytically active sites.[57] Due to the unique structure of keratin-protein-grafted graphene oxide nanosheets (KP–GO), use of KP–GO as support for covalent immobilization of PdTSPc prevents the aggregation of PdTSPc. Preventing of aggregation of PdTSPc is providing more active sites for the catalytic application. To prove this claim, the SEM and TEM images of prepared PdTSPc@KP–GO catalyst were provided. The SEM and TEM images of prepared PdTSPc@KP–GO catalyst in comparison with GO and KP–GO did not show any aggregation which confirmed the monomeric molecular dispersion of PdTSPc on the surface of KP–GO.

Raman spectroscopy, as a useful tool for investigating the electronic and phonon structure of graphene-based materials, was used to study the synthesized GO and PdTSPc@KP–GO. The Raman spectra of prepared GO and PdTSPc@KP–GO are shown in Fig. 7. Raman spectrum of GO shows two prominent peaks at 1578 and 1305 cm^{-1} related to G-band and D-band, respectively. The G-band is the result of the first-order scattering of the E_{2g} mode of sp^2 carbon domains and D-band is characteristic of a breathing mode for *k*-point phonons of A_{1g}. The characteristic D and G bands of PdTSPc@KP–GO are observed around 1312 and 1589 cm^{-1}, respectively, which indicate the D-band and G-band of GO.

The electronic property of PdTSPc@KP–GO nanocomposite was explored by X-ray photoelectron spectroscopy (XPS) analysis. As shown in Fig. 8, the peaks corresponding to C 1s, N 1s, O 1s, S 2s and 2p, and Pd 3s, 3p and 3d was clearly observed in the XPS survey spectrum. From the N 1s XPS scan shown in Fig. 8b, it is observed that two different types of nitrogen are present in the PdTSPc@KP–GO nanocomposite. The N 1s spectra could be divided into two peaks, one peak at 399.09 eV ascribed to sp^2 nitrogen in the phthalocyanine ring of the PdTSPc complex and another peak at 400.09 eV attributed to the aliphatic nitrogen of the keratin protein.[58,59] The S 2p spectrum of PdTSPc@KP–GO is shown in Fig. 8c. There are two kinds of S containing group, $–SO_3H$ and –S–S–, in PdTSPc@KP–GO, and their S 2p binding energies are different. The S 2p signal for PdTSPc@KP–GO nanocomposite includes two components. The first component located at 167.70 eV is attributable to –S–S– groups of the keratin protein.[59] The second one situated at 168.74 eV is attributed to $–SO_3H$ groups of PdTSPc.[59] The peaks at 338.09 and 343.35 eV are associated with palladium in the oxidation state of II in the PdTSPc@KP–GO nanocomposite which confirmed the +2 oxidation state of Pd in phthalocyanine ligand (Fig. 8d).[58]

For examination of the catalytic activity of the prepared PdTSPc@KP–GO precatalyst in C–C coupling reactions, Heck coupling of bromobenzene with styrene and Sonogashira coupling of bromobenzene with phenylacetylene were selected as model reactions. To optimize the required base and the amount of catalyst, the mentioned reactions were performed in H_2O as green reaction media and the results are summarized in Table 1. The comparison of the results related to the effect of the various amounts of PdTSPc@KP–GO precatalyst revealed that the 0.8 and 1.0 mol% of PdTSPc@KP–GO are providing the best result for Heck coupling of bromobenzene with styrene and Sonogashira coupling of bromobenzene with phenylacetylene, respectively. PdTSPc@KP–GO was found to give good yield with Heck coupling of bromobenzene with styrene (entry 1) and to be effective for Sonogashira coupling of bromobenzene with phenylacetylene (entry 8). Palladium tetrasulfophthalocyanine as a preference for the Pd(II) oxidation state has complete coordinative saturation of the central Pd atom and high chemical and thermal stability. The very rigid structure and extraordinarily high complex stability of PdTSPc lead to the very limited release of Pd when heated under coupling reaction conditions. Since Pd released by palladium tetrasulfophthalocyanine would be limited and completely unsaturated, PdTSPc is a very applicable model system to catalyze C–C coupling reactions.[12] On the other hand, PdTSPc remains thermally and chemically stable even under the harsh reaction conditions needed for the activation and conversion of demanding substrates.

GO shows good dispersity in water. Since graphene oxide is inert for chemically PdTSPc–graphene interactions, wool keratin protein as amphiphilic biomaterial with hydrophobic and hydrophilic segments in backbone or side groups was extracted from natural wool and used as "adhesive" to chemically link PdTSPc and graphene oxide. The keratin protein was added to the GO to make it suitable support to chemically immobilize the PdTSPc. The high dispersity of the catalytic system is essential for its high efficiency; therefore, the dispersity of the prepared catalytic system was studied in water (as reaction media) to evaluate its stability and dispersibility. The results showed that not only the dispersity of the prepared catalyst is not decreased but also, it was increased to some

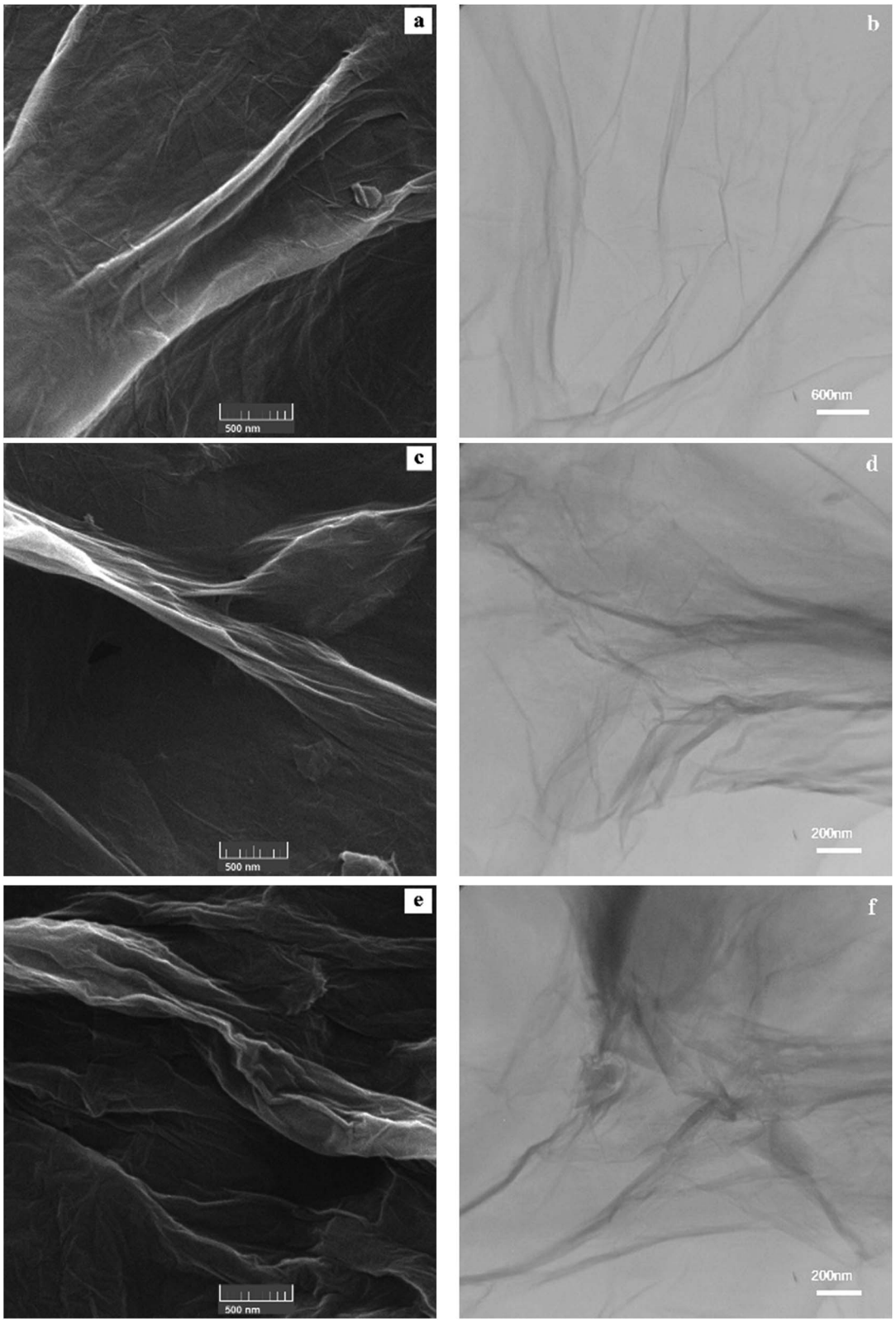

Fig. 6 SEM and TEM images of GO (a, b), KP–GO (c, d), and PdTSPc@KP–GO (e, f).

extent. Both of GO and PdTSPc@KP–GO showed good dispersity and stability in water, but PdTSPc@KP–GO is more dispersible and stable in long times (3 weeks). Use of keratin protein and aqua soluble palladium tetrasulfophthalocyanine increased the hydrophilic properties of the PdTSPc@KP–GO, which consequently the stability and dispersity of the precatalyst were

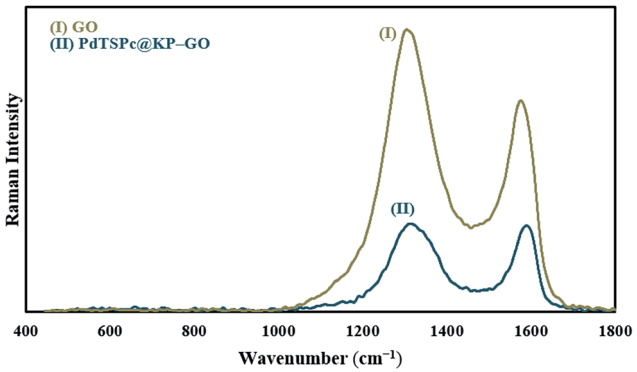

Fig. 7 Raman spectra of GO(I) and PdTSPc@KP–GO(II).

improved in aqueous solution (Fig. 9). In addition, by immobilization of the water soluble PdTSPc on the insoluble keratin-protein-grafted graphene oxide nanosheets *via* covalent attachment, the separation process of the homogeneous PdTSPc is simplified.

To show the role of the support in C–C coupling reactions, Heck coupling of bromobenzene with styrene and Sonogashira coupling of bromobenzene with phenylacetylene were accomplished using PdTSPc and PdTSPc@KP–GO under the same reaction conditions. The obtained results which are shown in Table 1 (entries 1, 7, 8, 14) showed that PdTSPc@KP–GO gave better conversions and it has higher catalytic activity than unsupported PdTSPc. It could be concluded that KP–GO enhance the catalytic activity of the prepared system in Heck and Sonogashira coupling reactions. Use of KP–GO as a support for covalent immobilization of PdTSPc can promote the adsorption of aromatic reactants because of the π–π interaction between graphene support and benzene skeleton of the reactants. Also, the good dispersity of PdTSPc@KP–GO in the aqueous solution as an important factor seems to enhance the efficiency of prepared precatalyst.

To examine the controlled temporary release of active species from PdTSPc@KP–GO in Heck coupling of styrene and bromobenzene, the catalyst was separated from reaction media after 9 h in two different conditions. Once immediately from the hot reaction media (100 °C) and another one after cooling the reaction mixture. Flame atomic absorption spectrometry (FAAS) method was used to determine the palladium content in the both of the solutions. The analysis of the hot and cooled residue solution was showed that the Pd content in the reaction media is 2.1 ppm and below 0.1 ppm, respectively, which it could be

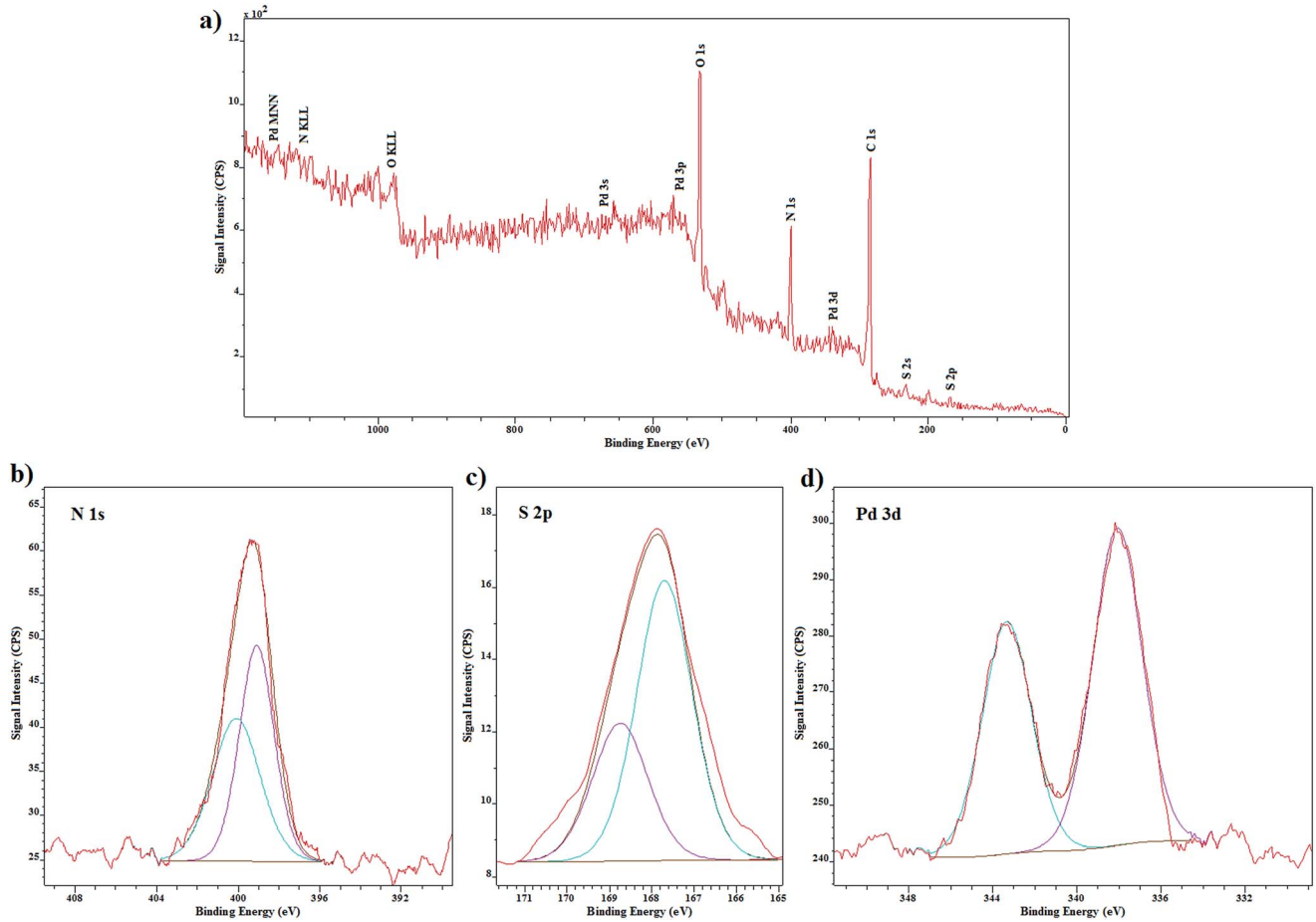

Fig. 8 (a) Full-range XPS spectrum of PdTSPc@KP–GO nanocomposite. (b) N 1s, (c) S 2p, (d) Pd 3d core-level region XPS spectra of PdTSPc@KP–GO nanocomposite.

Table 1 Optimization of the reaction conditions for the Heck coupling of bromobenzene with styrene and Sonogashira coupling of bromobenzene with phenylacetylene by PdTSPc@KP–GO precatalyst[a,b]

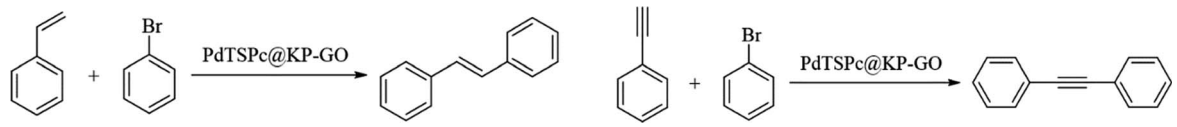

Entry	Amount of catalyst (Pd content/mol%)	Base	Yield[c]
1	98 mg (0.8)	K_2CO_3	87
2	86 mg (0.7)	K_2CO_3	71
3	74 mg (0.6)	K_2CO_3	42
4	98 mg (0.8)	Na_2CO_3	41
5	98 mg (0.8)	NaOAc	72
6	98 mg (0.8)	Et_3N	69
7[d]	8.0 mg (0.8)	K_2CO_3	53
8	123 mg (1.0)	K_2CO_3	85
9	111 mg (0.9)	K_2CO_3	64
10	98 mg (0.8)	K_2CO_3	49
11	123 mg (1.0)	Na_2CO_3	32
12	123 mg (1.0)	NaOAc	78
13	123 mg (1.0)	Et_3N	76
14[d]	10 mg (1.0)	K_2CO_3	45

[a] Reaction conditions for Heck coupling of bromobenzene with styrene (entries 1–7): bromobenzene (1.5 mmol), styrene (1.0 mmol), base (2.0 mmol), H_2O (10 mL), reflux, 9 h. [b] Reaction conditions for Sonogashira coupling of bromobenzene with phenylacetylene (entries 8–14): bromobenzene (2.0 mmol), phenylacetylene (1.0 mmol), CuI (4.0 mol%), base (2.0 mmol), H_2O (10 mL), reflux, 9 h. [c] GC yield, *n*-dodecane was used as an internal standard. [d] PdTSPc was used as precatalyst.

Fig. 9 Dispersity of GO and PdTSPc@KP–GO after 3 weeks.

concluded that release of Pd^{2+} active species from PdTSPc@KP–GO is reversible by cooling of reaction media. These observations are confirming the release of ligandless Pd^{2+} species in the hot reaction media. Because the equilibrium constant of the metal release from the complex is related to the temperature and the release of metal will be increased by increasing the temperature.[60–62] Therefore, the obtained results can be attributed to the increase of metal release from the complex by increasing the temperature.

Since, the optimized reaction conditions were achieved, the scope and limitation of the mentioned method were investigated for the Heck coupling of styrene and Sonogashira coupling of phenylacetylene with different aryl halides in the presence of 98 and 123 mg of PdTSPc@KP–GO as preferred amounts of precatalyst, respectively (Table 2). As expected, the catalytic activity of PdTSPc@KP–GO depended on the halide in the order ArCl < ArBr < ArI (entries 1–3 and 8–10). On the other hand, electron-withdrawing groups on the aryl halide ring increased the rate of reaction. As indicated in Table 2, after 9 h reaction time for Heck coupling of styrene with different bromobenzenes, the yield of the coupling product was found to be 80% for deactivated 4-bromoanisole (entry 4), 87% for non-activated bromobenzene (entry 2), and 99% for activated 4-bromonitrobenzene (entry 6).

To examine the leaching of PdTSPc from PdTSPc@KP–GO, in Heck coupling of styrene and bromobenzene, the catalyst was removed by filtration after ~30% conversion. The residue was applied to further treatment under similar reaction conditions for 24 h. After determination of the conversion by GC method, the obtained results showed that the reaction did not proceed and no coupling product was detected. Also, FAAS shows that the palladium content in the residue solution is below 0.1 ppm which leaching in the PdTSPc@KP–GO catalyst is negligible. With respect to the mentioned results, it could be concluded that excellent heterogeneity is displayed by PdTSPc@KP–GO.

In Table 3, the results of our investigations have been compared to previous reports of graphene-based palladium complex catalysts.[14–20,63] The main advantages of the present system in comparison with the previous graphene-based palladium complex catalysts are the controlled and reversible release of the Pd from the precatalyst. The reversible release of the Pd

Table 2 The Heck coupling of aryl halides with styrene and Sonogashira coupling of aryl halides with phenylacetylene by PdTSPc@KP–GO precatalyst[a,b]

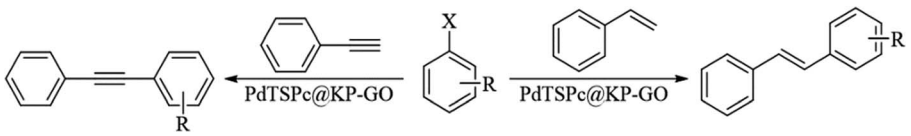

Entry	R/X	Substrate	Yield[c]	TON/TOF (h^{-1})
1[d]	H/Cl	Styrene	25	31.2 (3.47)
2	H/Br	Styrene	87	108.7 (12.08)
3	H/I	Styrene	89	111.2 (12.36)
4	4-CH_3/Br	Styrene	80	100.0 (11.11)
5	4-CH_3/I	Styrene	85	106.2 (11.80)
6	4-NO_2/Br	Styrene	99	123.7 (13.75)
7	4-NO_2/I	Styrene	99	123.7 (13.75)
8[d]	H/Cl	Phenylacetylene	33	33.0 (3.66)
9	H/Br	Phenylacetylene	85	85.0 (9.44)
10	H/I	Phenylacetylene	88	88.0 (9.77)
11	4-CH_3/Br	Phenylacetylene	79	79.0 (8.77)
12	4-CH_3/I	Phenylacetylene	83	83.0 (9.22)
13	4-NO_2/Br	Phenylacetylene	95	95.0 (10.55)
14	4-NO_2/I	Phenylacetylene	94	94.0 (10.44)

[a] Reaction conditions for Heck coupling of aryl halides with styrene: aryl halide (1.5 mmol), styrene (1.0 mmol), PdTSPc@KP–GO (98 mg), K_2CO_3 (2.0 mmol), H_2O (10 mL), reflux, 9 h. [b] Reaction conditions for Sonogashira coupling of aryl halides with phenylacetylene: aryl halide (2.0 mmol), phenylacetylene (1.0 mmol), PdTSPc@KP–GO (123 mg), K_2CO_3 (2.0 mmol), CuI (4.0 mol%), H_2O (10 mL), reflux, 9 h. [c] GC yield, *n*-dodecane was used as an internal standard. [d] Reaction time: 48 h.

makes it possible to reuse the catalyst. Also, irreversible precipitation of palladium in the reaction media, which affected its catalytic activities, is prevented by controlled and reversible release of palladium from macrocyclic phthalocyanine complex. The interplay between the release and recoordination of Pd in the phthalocyanine ligand is the reason for high catalytic performances of PdTSPc@KP–GO as precatalyst in C–C coupling reactions. Furthermore, the use of green keratin protein to chemically attaching of the PdTSPc is providing the green and recyclable catalyst.

Recyclability of the PdTSPc@KP–GO precatalyst was examined in the Heck coupling of styrene and bromobenzene. Accordingly, PdTSPc@KP–GO catalyst was separated from reaction media by centrifuging, dried under vacuum at 60 °C, and reused for five repetitive cycles in the mentioned reaction. As indicated in Fig. 10, the results show that only minor decreases in the reaction yields are observable; it means that the activity and efficiency of the catalyst were saved during successive uses due to the high stability of PdTSPc@KP–GO under the reaction conditions.

Table 3 Comparison of the results obtained from graphene-based palladium complex catalysts for the C–C coupling reactions

Entry	Reaction	Catalyst	Conditions	Molar ratio substrate to catalyst	Recyclability	Ref.
1	Suzuki reaction	GO–NHC–Pd	DMF–H_2O/Cs_2CO_3/50 °C/1 h	1 : 0.0100	5 runs	14
2	Suzuki reaction	GO–NHC–Pd^{2+}	EtOH–H_2O/K_2CO_3/80 °C/1–24 h	1 : 0.0025	6 runs	15
3	Suzuki reaction	NHC–Pd/GO–IL	EtOH–H_2O/K_2CO_3/60 °C/2.5 h	1 : 0.0010	5 runs	16
4	Heck reaction	Pd@AGu@MGO	EtOH–H_2O/K_2CO_3/r.t./2.5 h	1 : 0.0090	20 runs	17
5	Suzuki reaction	Pd@AGu@MGO	H_2O/K_2CO_3/r.t./2.5 h	1 : 0.0090	20 runs	17
6	Heck reaction	Pd(II)–FRGO	DMF/Et_3N/100–120 °C/10 or 20 h	1 : 0.0100	4 runs	63
7	Suzuki reaction	Pd(II)–FRGO	EtOH–H_2O/Na_2CO_3/r.t./8 h	1 : 0.0025	4 runs	63
8	Suzuki reaction	GO–2N–Pd(II)	EtOH/K_2CO_3/80 °C/0.5–20 h	1 : 0.0050	6 runs	18
9	Heck reaction	TRGO–NPy–Pd	DMF/Na_2CO_3/140 °C/1.5–21 h	1 : 0.0030	8 runs	19
10	Suzuki reaction	Co/C–ROMPgel immobilized Pd-complex	THF–H_2O/Na_2CO_3/65 °C/2–12 h	1 : 0.0110	7 runs	20
11	Heck reaction	PdTSPc@KP–GO	H_2O/K_2CO_3/ref./9 h	1 : 0.0080	5 runs	This work
12	Sonogashira reaction	PdTSPc@KP–GO	H_2O/K_2CO_3/ref./9 h	1 : 0100	—	This work

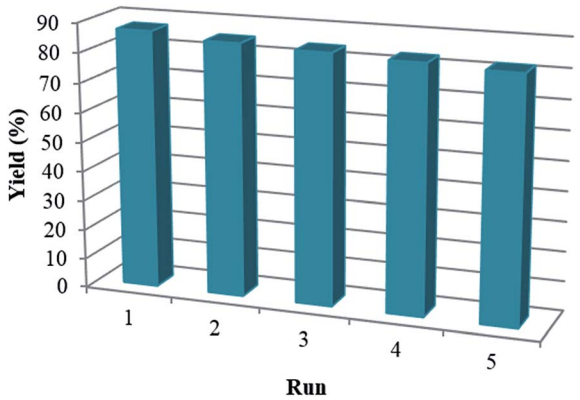

Fig. 10 Successive use of the prepared PdTSPc@KP–GO precatalyst for the Heck coupling of styrene and bromobenzene.

Conclusion

Wool keratin protein was extracted from natural wool and the extracted protein was used to modify the surface of graphene oxide nanosheets and preparation of KP–GO. Aqua soluble palladium(II) tetrasulfophthalocyanine, which has ability to be attached covalently, was supported on KP–GO. In continue, the efficient palladium(II) tetrasulfophthalocyanine catalyzed method was developed for the C–C coupling in Heck and Sonogashira reactions in H_2O as the reaction media using PdTSPc@KP–GO as precatalyst. PdTSPc@KP–GO precatalyst showed high C–C coupling activity in Heck and Sonogashira reactions because of controlled *in situ* release of catalytic active palladium species by stable and inactive PdTSPc@KP–GO precursor. PdTSPc in the PdTSPc@KP–GO precatalyst releases only very low amounts of palladium into the solution which lead to high activities in C–C coupling reactions. By covalent immobilization of water soluble PdTSPc on KP–GO, not only the stability and dispersity of the precatalyst were improved in aqueous solution but the separation of the homogeneous PdTSPc precatalyst from H_2O as the reaction media was simplified.

Acknowledgements

We gratefully acknowledge financial support from the Iran National Elites Foundation (INEF) and the Research Council of Shahid Beheshti University.

Notes and references

1 N. Miyaura and A. Suzuki, *Chem. Rev.*, 1995, **95**, 2457–2483.
2 K. J. Bonney and F. Schoenebeck, *Chem. Soc. Rev.*, 2014, **43**, 6609–6638.
3 R. Chinchilla and C. Nájera, *Chem. Soc. Rev.*, 2011, **40**, 5084–5121.
4 A. Fihri, M. Bouhrara, B. Nekoueishahraki, J.-M. Basset and V. Polshettiwar, *Chem. Soc. Rev.*, 2011, **40**, 5181–5203.
5 Q. Wang, Y. Su, L. Li and H. Huang, *Chem. Soc. Rev.*, 2016, **45**, 1257–1272.
6 J. M. Pérez, R. Cano, G. P. McGlacken and D. J. Ramón, *RSC Adv.*, 2016, **6**, 36932–36941.
7 P. Wójcik, M. Mart, S. Ulukanli and A. M. Trzeciak, *RSC Adv.*, 2016, **6**, 36491–36499.
8 S. Elavarasan, B. Baskar, C. Senthil, P. Bhanja, A. Bhaumik, P. Selvam and M. Sasidharan, *RSC Adv.*, 2016, **6**, 49376–49386.
9 I. D. Kostas, A. G. Coutsolelos, G. Charalambidis and A. Skondra, *Tetrahedron Lett.*, 2007, **48**, 6688–6691.
10 Q.-X. Wan and Y. Liu, *Catal. Lett.*, 2008, **128**, 487–492.
11 C. Röhlich and K. Köhler, *Chem.–Eur. J.*, 2010, **16**, 2363–2365.
12 C. Röhlich and K. Köhler, *Adv. Synth. Catal.*, 2010, **352**, 2263–2274.
13 A. B. Sorokin, *Chem. Rev.*, 2013, **113**, 8152–8191.
14 J. H. Park, F. Raza, S.-J. Jeon, H.-I. Kim, T. W. Kang, D. Yim and J.-H. Kim, *Tetrahedron Lett.*, 2014, **55**, 3426–3430.
15 N. Shang, S. Gao, C. Feng, H. Zhang, C. Wang and Z. Wang, *RSC Adv.*, 2013, **3**, 21863–21868.
16 S. K. Movahed, R. Esmatpoursalmani and A. Bazgir, *RSC Adv.*, 2014, **4**, 14586–14591.
17 L. Ma'mani, S. Miri, M. Mahdavi, S. Bahadorikhalili, E. Lotfi, A. Foroumadi and A. Shafiee, *RSC Adv.*, 2014, **4**, 48613–48620.
18 C. Bai, Q. Zhao, Y. Li, G. Zhang, F. Zhang and X. Fan, *Catal. Lett.*, 2014, **144**, 1617–1623.
19 L. Fernández-García, M. Blanco, C. Blanco, P. Álvarez, M. Granda, R. Santamaría and R. Menéndez, *J. Mol. Catal. A: Chem.*, 2016, **416**, 140–146.
20 A. Schätz, T. R. Long, R. N. Grass, W. J. Stark, P. R. Hanson and O. Reiser, *Adv. Funct. Mater.*, 2010, **20**, 4323–4328.
21 J. Yang, D. Mu, Y. Gao, J. Tan, A. Lu and D. Ma, *J. Nat. Gas Chem.*, 2012, **21**, 265–269.
22 J.-H. Yang, Y. Gao, W. Zhang, P. Tang, J. Tan, A.-H. Lu and D. Ma, *J. Phys. Chem. C*, 2013, **117**, 3785–3788.
23 M. Mahyari and A. Shaabani, *Appl. Catal., A*, 2014, **469**, 524–531.
24 M. Mahyari, M. S. Laeini and A. Shaabani, *Chem. Commun.*, 2014, **50**, 7855–7857.
25 K. Hu, M. K. Gupta, D. D. Kulkarni and V. V. Tsukruk, *Adv. Mater.*, 2013, **25**, 2301–2307.
26 A. Shaabani, Z. Hezarkhani and S. Shaabani, *RSC Adv.*, 2014, **4**, 64419–64428.
27 A. Shaabani, Z. Hezarkhani and E. Badali, *RSC Adv.*, 2015, **5**, 61759–61767.
28 A. Shaabani, Z. Hezarkhani and E. Badali, *Polyhedron*, 2016, **107**, 176–182.
29 A. Idris, R. Vijayaraghavan, U. A. Rana, A. F. Patti and D. R. MacFarlane, *Green Chem.*, 2014, **16**, 2857–2864.
30 A. J. Poole, J. S. Church and M. G. Huson, *Biomacromolecules*, 2009, **10**, 1–8.
31 K. Yamauchi, A. Yamauchi, T. Kusunoki, A. Kohda and Y. Konishi, *J. Biomed. Mater. Res.*, 1996, **31**, 439–444.
32 E.-K. Bang, M. Lista, G. Sforazzini, N. Sakai and S. Matile, *Chem. Sci.*, 2012, **3**, 1752–1763.
33 *The Porphyrin Handbook*, ed. K. M. Kadish, K. M. Smith and R. Guilard, Academic Press, Amsterdam, 2002.
34 H. J. Rhodes, B. Potter and A. Widra, *Mycopathol. Mycol. Appl.*, 1967, **33**, 345–348.

35 R. Cecil and J. R. Mcphee, *Advances in Protein Chemistry*, Academic Press, New York and London, 1959.
36 R. S. Asquith, *Chemistry of Natural Protein Fibers*, Springer, US, New York, 1977.
37 S. Sabater, J. A. Mata and E. Peris, *ACS Catal.*, 2014, **4**, 2038–2047.
38 Y. Huang, Z. Ma, Y. Hu, D. Chai, Y. Qiu, G. Gao and P. Hu, *RSC Adv.*, 2016, **6**, 51725–51731.
39 L.-N. Zhou, X.-T. Zhang, W.-J. Shen, S.-G. Sun and Y.-J. Li, *RSC Adv.*, 2015, **5**, 46017–46025.
40 H. Fan, L. Wang, K. Zhao, N. Li, Z. Shi, Z. Ge and Z. Jin, *Biomacromolecules*, 2010, **11**, 2345–2351.
41 P. Zheng, T. Ma and X. Ma, *Ind. Eng. Chem. Res.*, 2013, **52**, 14201–14207.
42 C. Zhang, R. Z. Zhang, Y. Q. Ma, W. B. Guan, X. L. Wu, X. Liu, H. Li, Y. L. Du and C. P. Pan, *ACS Sustainable Chem. Eng.*, 2015, **3**, 396–405.
43 C. Rodríguez-González, A. L. Martínez-Hernández, V. M. Castaño, O. V. Kharissova, R. S. Ruoff and C. Velasco-Santos, *Ind. Eng. Chem. Res.*, 2012, **51**, 3619–3629.
44 S. Xu, L. Yong and P. Wu, *ACS Appl. Mater. Interfaces*, 2013, **5**, 654–662.
45 A. Shaabani, *J. Chem. Res.*, 1998, 672–673.
46 H. Mofakham, Z. Hezarkhani and A. Shaabani, *J. Mol. Catal. A: Chem.*, 2012, **360**, 26–34.
47 A. Shaabani, Z. Hezarkhani and M. K. Nejad, *RSC Adv.*, 2016, **6**, 30247–30257.
48 A. Shaabani and Z. Hezarkhani, *Cellulose*, 2015, **22**, 3027–3046.
49 M. Seyyedhamzeh, N. Ganji and A. Shaabani, *J. Porphyrins Phthalocyanines*, 2012, **16**, 1110–1113.
50 A. Feofanov, A. Grichine, T. Karmakova, N. Kazachkina, E. Pecherskih, R. Yakubovskaya, E. Luḱyanets, V. Derkacheva, M. Egret-Charlier and P. Vigny, *Photochem. Photobiol.*, 2007, **75**, 527–533.
51 J. William, S. Hummers and R. E. Offeman, *J. Am. Chem. Soc.*, 1958, **80**, 1339.
52 N. I. Kovtyukhova, P. J. Ollivier, B. R. Martin, T. E. Mallouk, S. a. Chizhik, E. V. Buzaneva and A. D. Gorchinskiy, *Chem. Mater.*, 1999, **11**, 771–778.
53 T. Yang, L. Liu, J. Liu, M.-L. Chen and J.-H. Wang, *J. Mater. Chem.*, 2012, **22**, 21909–21916.
54 D. C. Marcano, D. V. Kosynkin, J. M. Berlin, A. Sinitskii, Z. Sun, A. Slesarev, L. B. Alemany, W. Lu and J. M. Tour, *ACS Nano*, 2010, **4**, 4806–4814.
55 K. Wang, R. Li, J. H. Ma, Y. K. Jian and J. N. Che, *Green Chem.*, 2016, **18**, 476–481.
56 A. Muñoz García, A. J. Hunt, V. L. Budarin, H. L. Parker, P. S. Shuttleworth, G. J. Ellis and J. H. Clark, *Green Chem.*, 2015, **17**, 2146–2149.
57 Y. Jiang, Y. Lu, X. Lv, D. Han, Q. Zhang, L. Niu and W. Chen, *ACS Catal.*, 2013, **3**, 1263–1271.
58 K. S. Lokesh and A. Adriaens, *Dyes Pigm.*, 2013, **96**, 269–277.
59 S. Wu, H. Ma, X. Jia, Y. Zhong and Z. Lei, *Tetrahedron*, 2011, **67**, 250–256.
60 J. H. Flynn, *J. Therm. Anal.*, 1990, **36**, 1579–1593.
61 R. Larsson, L. Y. Johansson and L. Jonsson, *J. Appl. Electrochem.*, 1981, **11**, 489–492.
62 M. Beyrhouty, A. B. Sorokin, S. Daniele and L. G. Hubert-Pfalzgraf, *New J. Chem.*, 2005, **29**, 1245–1248.
63 S. Wang, D. Hu, W. Hua, J. Gu, Q. Zhang, X. Jia and K. Xi, *RSC Adv.*, 2015, **5**, 53935–53939.